Evaluation of the Impact of High Bandwidth Energy Storage Systems on DC Protection

Puran Rakhra, Patrick J. Norman, Steven D. A. Fletcher, *Member, IEEE,* Stuart J. Galloway and
Graeme M. Burt, *Member, IEEE*

Abstract—The integration of high bandwidth energy storage systems (ESS) in compact DC electrical power systems can increase the operational capability and overall flexibility of the network. However, the impact of ESSs on the performance of existing DC protection systems is not well understood. This paper identifies the key characteristics of the ESS that determine the extent of the protection blinding effects on slower acting generator systems on the network. It shows that higher fault impedances beyond that of an evaluated critical level will dampen the response of slower acting generator systems, decreasing the speed of corresponding overcurrent protection operation. The paper demonstrates the limitations of existing protection solutions and identifies more suitable protection approaches to remove/minimize the effects of protection blinding.

Index Terms—Compact dc power systems, Fault conditions, High bandwidth energy storage, protection.

I. INTRODUCTION

HIGH BANDWIDTH, power-dense energy storage systems (ESS) with highly dynamic charge/discharge characteristics are being considered to perform increasingly demanding roles and complex network functions in DC power system applications. These include providing backup power, meeting peak load demand and maintaining power quality during variable load conditions or switching events. Candidate ESS technologies that meet the bandwidth and power rating requirements to perform these functions include supercapacitor and flywheel energy storage systems [1]. Applications include microgrids [2-4], shipboard systems [5-7] and aircraft systems [8]. Such functionality can increase overall system efficiency, provide better transient performance, potentially reduce primary generation capacity and increase security of supply [9].

To date the emphasis within the academic literature has focused on the benefits of integrating versatile ESS. However, the systems-level impact that energy storage may have during abnormal operating conditions is not well understood. The authors have previously highlighted that the inherent ESS response to electrical faults on a DC network has the potential to impair the performance of upstream protection [10, 11]. In particular, the contribution of fault current from an ESS may cause protection blinding, which is known to affect the performance of non-unit protection methods [12, 40].

This paper evaluates the impact of high-bandwidth ESSs on the performance of conventional network-wide protection in compact dc power systems. It gives clear guidance to network designers as to which conditions the ESS may degrade protection system performance and when it may improve it. A number of variables are considered including: ESS controller bandwidth (i.e. its response time to changing conditions), fault impedance, connection state, the state of charge (SOC) and the peak current output. The relative importance and impact of these factors are determined through numerous simulations conducted on a DC power system model. The paper concludes by identifying potential protection approaches capable of minimizing or eliminating the protection blinding effects.

II. STATE OF THE ART IN DC PROTECTION SYSTEMS

DC faults can pose exceptionally demanding protection challenges in terms of speed of propagation and fault current magnitude in comparison to faults within AC systems [13, 15]. These issues are strongly driven by the behavioral characteristics of standard voltage source converters, used for rectification in DC networks, under fault conditions. These are namely: the inability to limit fault current and the relatively low fault tolerance of the converters [13, 15].

Increasingly popular solutions to overcome these limitations include the redesign of the converter to be more fault tolerant and the use of converter based current limiting to suppress fault [17, 26, 27]. The use of converter current limiting potentially reduces the speed requirements of the protection system enabling the continued use of standard AC side circuit breakers or electromechanical DC switchgear for fault clearance [17-23].

Whilst beneficial from a converter protection perspective, the use of current limiting can make the coordination of network protection more challenging as fault current may be similar for many fault locations (particularly in compact, low resistance networks). This leads protection in these systems to typically be time-graded with respect to the output of the current limiting converter interface [17-23]. The main disadvantage of this approach is a slower operating speed due to the need to set an operating delay between coordinating protection devices. This increase in operating time can have significant consequences for energy delivered at the point of

The authors are with the Institute for Energy and Environment, Department of Electronic and Electrical Engineering, University of Strathclyde, Glasgow G1 1XW, U.K. (e-mail: puran.rakra@strath.ac.uk; patrick.norman@.strath.ac.uk; steven.fletcher@strath.ac.uk;; stuart.galloway@strath.ac.uk; graeme.burt@strath.ac.uk)

fault, particularly for arcing faults [24, 25]. Later section of this paper will also demonstrate how the integration of energy storage can also influence this protection operating speed in current limiting environments, an issue not yet reflected in current literature.

State-of-the-art programmable solid state protection devices [27, 28] can offer greater flexibility in enabling effective coordination. However, commercial devices still employ slow i^2t protection algorithms and are only designed for load protection functionality. A more distributed solid-state protection device test bed has been demonstrated in [27], where additional restraint signals between devices have been proposed to improve protection coordination. However, considerable work is still required to verify the viability of solid-state devices to provide network-wide DC protection.

III. INTEGRATION CHALLENGES OF HIGH BANDWIDTH ENERGY STORAGE SYSTEMS

Two key and often complimentary functions of ESS within compact power systems are to ensure that load demand is met and that network power quality is maintained [3, 5, 29]. High-bandwidth converter interfaces operating in voltage control mode are key technological enablers for providing such functionality [30-32]. Accordingly, common control functions such as voltage transient mitigation can be achieved by exporting or absorbing power to or from the network to minimize the impact of transients. These control modes can however lead to significant implementation challenges during network fault conditions. In particular, the response of lower bandwidth sources (such as generators) during high-impedance faults can be significantly dampened, owing to the coupling that exists between sources via the network voltage.

To illustrate the impact this may have on the protection system, consider Fig. 1 which depicts an ESS connected to a DC power system via a converter interface. The potential control modes are identified: power quality regulation which acts on fast voltage transients, voltage support for slower variations in network voltage and SOC control. Under normal operating conditions, the ESS controller will regulate the ESS current output using the measurement of the network voltage, as in [33]. In the event of a network fault (such as that applied in Fig. 1), the subsequent reduction of network voltage will trigger a large step in its current reference value and drive the output of the current regulator into saturation (100% duty cycle). This will likely cause the ESS to continuously output current into the fault (provided that sufficient stored energy is available to support this and that the power electronic switches withstand the increase in current).

The subsequent damped response of the generator system to the fault may reduce the operational speed of its corresponding overcurrent protection device, causing protection blinding [12] and disrupting protection coordination. This will be demonstrated within this paper. A delay in upstream protection operating times may have detrimental effects on the system such as increasing energy delivered at the point of fault (if cleared by the generator protection device) and increasing time of fault exposure. This may be particularly hazardous in
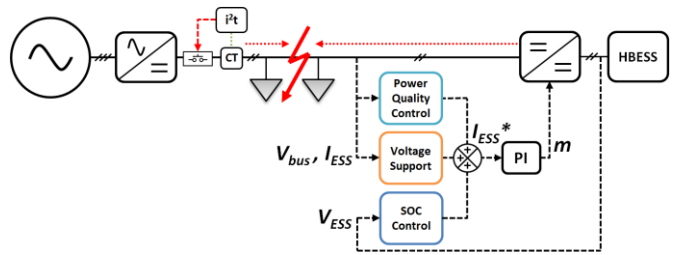

Fig. 1. Energy storage system controller

the event of arcing faults [24, 25] resulting in increased fire risk. Furthermore, the magnitude and direction of fault currents measured by the network-wide protection system will vary with ESS availability, changing the fault conditions.

These systems-level integration challenges have received little attention in current literature. For example [3] and [5] demonstrate the use of ESS to automate power balancing and for voltage sag correction during ac grid side faults on a microgrid. However, the response of these operational modes is not investigated during more severe faults within the DC microgrid. Furthermore, the protection challenges and requirements under such faulted conditions are not discussed.

Reference [34] considers the use of energy storage for fault ride-through of generator phase faults however provides no analysis for how similar ESS control would respond for electrical network faults. Reference [30] conducts fault studies for a low voltage DC microgrid containing battery storage, where commercial circuit breaker technology is suggested for protecting the battery during network faults. However, the protection selectivity challenges associated with such DC protection devices may cause the ESS protection to operate for faults at various downstream locations, unnecessarily disconnecting the ESS. Similar drawbacks associated with grid connected ESSs are highlighted in [35] where a superconducting fault current limiter is proposed to minimise protection coordination issues caused by the ESS whilst maintaining the availability of the ESS for post fault recovery. However, the cost and complexities of implementing such systems may limit their use in certain applications.

The evidence therefore suggests that the compatibility of existing network protection systems with networks containing fast acting and power-dense ESS is not well understood. To fully evaluate ESS impact on the protection performance, the technical characteristics of the ESS that govern the coupled behaviour of paralleled sources (through the network voltage) must be assessed. The two key behavioral characteristics of ESS which influence this are described below.

First, the maximum sustained current output from the ESS will determine its ability to support the network voltage. This peak current may be due to the storage device itself or its converter interface (assuming current limiting capability). It may be rated to output a maximum current close to that of the demand from a peak load on the network, or limited to a fixed level to prevent physical damage to internal components [29].

Second, the speed of response of the ESS will determine its ability to respond to transient voltage changes. This is dictated by its internal impedance and the converter's closed-loop bandwidth, which takes into account the switching frequency
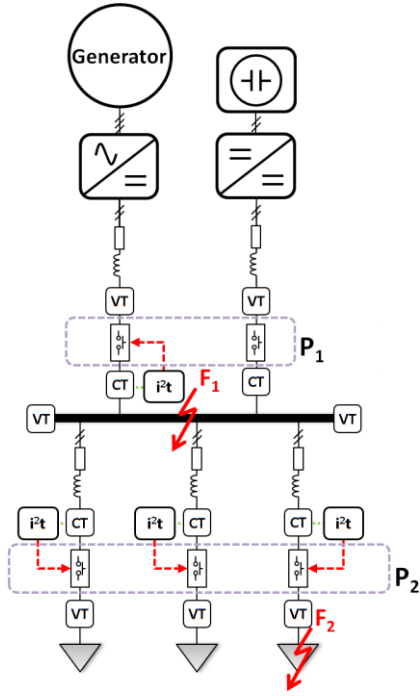
Fig. 2. DC compact power system with integrated ESS and a conventional overcurrent protection system

TABLE I
NETWORK PARAMETERS BASED ON A 270V DC POWER SYSTEM

Voltage (V)	Max Gen Current (A)	Max ESS Current (A)	R_{cab} (mΩ/ m)	L_{cab} (µH/ m)	Total P_{load} (kW)	Gen BW (kHz)	ESS BW (kHz)
270	200	200	0.272	0.65	19.9	1	100

Fig. 3. (a) Voltage response and (b) ESS/generator response to a low-impedance fault at F_1

of its converter interface and its controller gains [31, 33, 36]. To fulfill its potential for mitigating transient propagation, the ESS by its nature should be designed to respond rapidly to voltage transients. It should therefore operate at a higher bandwidth than that of the primary sources. Therefore in the event of a fault, the response of the ESS will likely impact the initial fault behavior of other connected sources and the subsequent protection response.

The following sections will illustrate the impact of the ESS on the fault response of the primary generation system for various fault scenarios, considering both changes in ESS behavioural characteristics and network fault conditions. Subsequent sections then derive relationships between these behavioural (designed) and conditional (variable) characteristics to identify the scenarios where protection performance is degraded.

IV. IMPACT OF ESS OPERATION ON FAULT AND PROTECTION RESPONSE OF GENERATOR SYSTEM

A key design objective of any network protection system is to safely provide continuity of supply to loads when other parts of the network are experiencing faults. The ability of the system to achieve this is measured using various performance criteria including speed, dependability and security [41]. The capability to provide backup protection in the event of a device failure is also taken into consideration. As a key contribution of this paper is to demonstrate the impact ESS integration has on the speed of generator feeder protection,
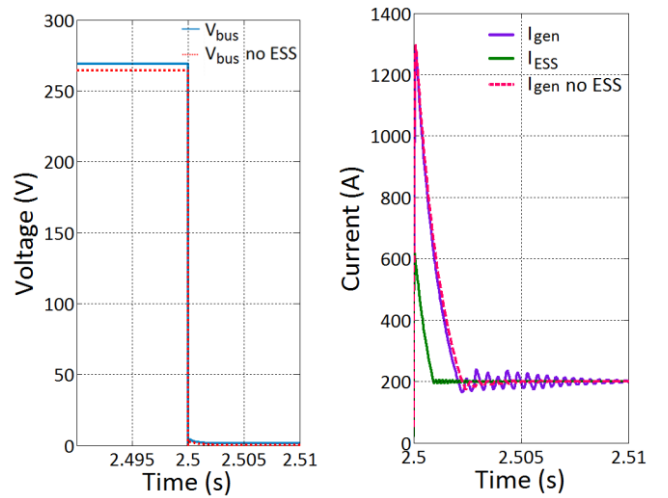
protection operating speed will be the main focus of the analysis within this section. However the section will also discuss how changes in operating speed have a corresponding impact on the dependability and security of generator protection.

Fig. 2 illustrates an example compact DC power system and Table I presents the relevant network parameters derived from a representative aircraft electrical system [14]. The system consists of a generation system and supercapacitor ESS connected in parallel to a common 270V DC bus bar via their respective converter interface. The conventional protection system for this tiered network architecture will normally consist of individual overcurrent relays that, in the event of a fault, must operate in a coordinated manner such that only the device immediately upstream from the fault operates [37]. Devices in parallel branches, i.e. in P_2 will be configured to operate within the same timeframe. The power system must also be designed to operate during periods when the ESS is disconnected or experiences depleted SOC. Consequently, the generator protection performance must be comparable for all cases. In order to evaluate the fault response of the power system and the inferred operation of conventional overcurrent protection devices, multiple simulations using a model of the DC power system described in Fig. 2 (developed in the MATLAB/Simulink environment [38]) were conducted.

The following case study only considers the fault response of the network shown in Fig. 2 for faults located at F_1. For faults located at F_2, it is anticipated that the speed of the adjacent overcurrent protection device will increase due to the additional fault current supplied by the ESS. A baseline study first operates the generator in isolation to characterize its fault response for a variety of fault impedances. These fault conditions are then replicated with the ESS connected and operational in order to illustrate the extent of protection blinding (decrease in speed) caused by the ESS. Within this initial study, the ESS has a nominal closed-loop bandwidth two orders of magnitude greater than that of the generator and its respective controller/converter interface. It is also assumed that both converters can current limit and this limit is
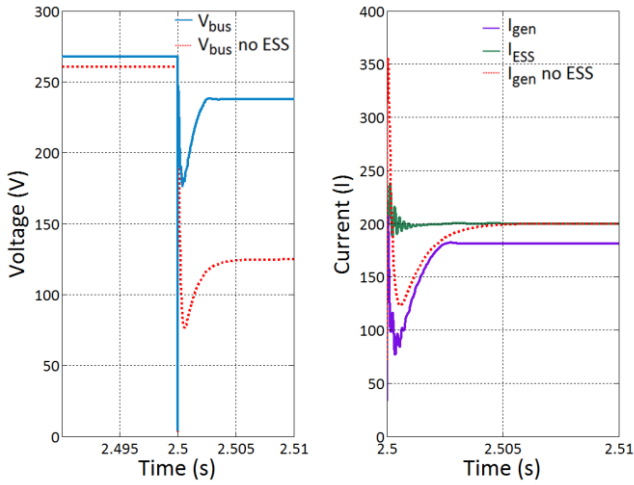
Fig. 4. (a) Voltage response and (b) ESS/generator response to a high-impedance fault at F_1

Fig. 5. Steady state i^2t response for increasing fault impedances at F_1 with (a) no ESS and (b) with ESS

nominally set to 200A. Subsequent studies will then explore the effects of varying the ESS current limit and ESS bandwidth on the protection system performance.

A. Impact of ESS response on current and voltage response of generator system

Fig. 3(a) and 3(b) show the simulated voltage response and corresponding ESS/generation system response to a low-impedance (1mΩ) fault applied after 2.5 seconds of simulation time (with no system protection). For both configurations (ESS operational/disconnected), the network voltage collapses rapidly to zero upon fault inception due to the discharge of DC side filter capacitance. When operational, the ESS response saturates at its peak current rating of 200A whilst the response of the generator system reaches its rated maximum of 200A for both configurations. The initial generator system peak current transient is produced by the discharge of its filter capacitor and is also similar in both cases. Given these similarities in both transient and steady state response it can be said that the ESS has minimal impact on the response of the generator system during low impedance faults.

Fig. 4(a) and 4(b) show the voltage response and ESS/generator system response to a high-impedance (750mΩ) fault at F_1. When the ESS is operational, a transient undervoltage event again occurs, causing the ESS to rapidly increase its current output to support the network voltage. The dominant ESS contribution of fault current (which again saturates to its maximum level) significantly reduces the depth of the undervoltage. This results in an initially reduced transient current output from the generator system. If the current traces are extended, the current output will eventually increase to its steady state saturation limit. Fig. 4(a) and (b) also illustrate the system behavior when the ESS is disconnected. In this case, the peak generator fault current is reached more rapidly. In the absence of the ESS, the fault-related voltage transient is far more significant in terms of both magnitude and duration. Consequently, any conventional generator protection device that operates on a function of the fault current will likely observe reduced fault current as a result of ESS integratio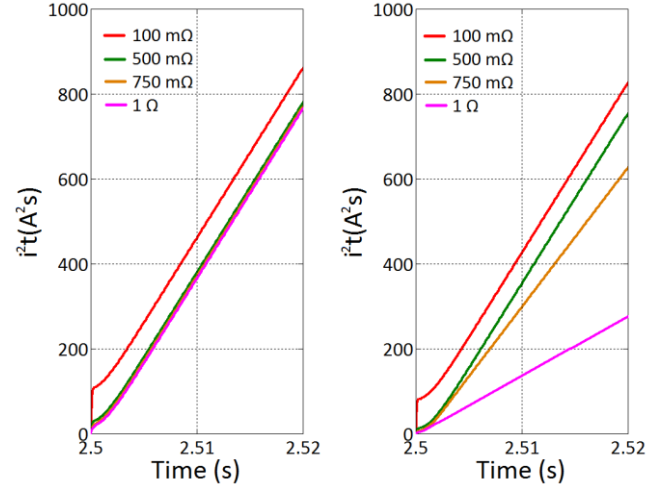n, causing protection blinding under high-impedance fault conditions. This will likely decrease the speed of conventional generator protection operation, prolong exposure of other electrical subsystems on the network to the fault and potentially compromise the safety of the power system with increased fire risk at the point of fault.

To quantify the conditions under which this impact exists, the following study assesses the fault energy (i^2t) the generator system delivers for a number of scenarios.

B. Impact of fault impedance and ESS on the fault energy output of the generator system

The relationship between the fault impedance and the degree of protection blinding caused by the response of the ESS can be determined by investigating the impact on the fault energy (i^2t) delivered from the generator system for various fault impedances. Fig. 5 and Fig. 6 present a range of simulation results that show the i^2t output of the generator system for increasing fault impedances located at F_1 on the network in Fig. 2. The impact of the ESS contribution on the generator system response is illustrated separately within Fig. 5(a) and (b), whereas both sets of traces are contrasted within Fig. 6 to compare the initial transient behavior of the i^2t response over a shorter timeframe.

From these figures, it can be seen that the influence of the ESS serves to progressively reduce the fault current from the generator system for increasing fault impedances. During lower impedance faults (up to 500mΩ), the output of the generator system is limited according to the rated current output of the converter. In these cases the contribution of the ESS only has the effect of shifting the i^2t curve associated with the generator and converter along the time axis during the initial fault transient. This would introduce an inconsequential small increase in trip-time in reaching a specified overcurrent threshold. However, for higher impedance faults, the contribution from the ESS actually serves to reduce the steady state gradient of the generator system output i^2t curve. This effect could significantly increase the trip-time of any associated protection devices.

To highlight how this trip time can be extended, the i^2t response can be compared to relevant operating thresholds.
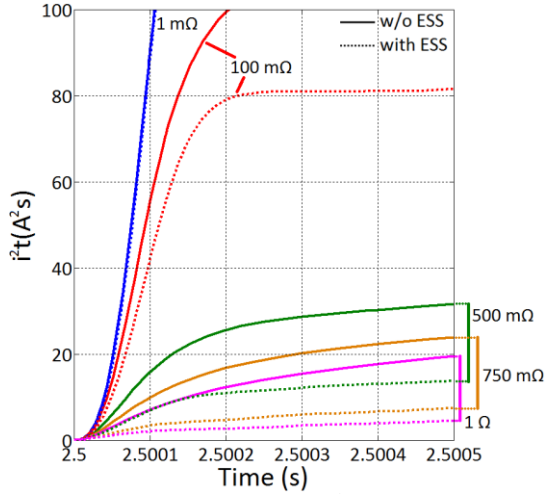
Fig. 6. Transient period generator system i^2t response for increasing fault impedances

Fig. 7. Generator system i^2t response for 750mΩ at F_1 with variable ESS current limit

Table II presents some examples of the time-to-threshold that are expected for the generator system operating as the single source of fault current, and operating in tandem with the ESS. The results show that for greater i^2t thresholds the increase in time, as a result of the ESS contribution to the fault, becomes significantly greater with increasing fault impedance. These are consistent with previous observations in Fig. 5 and 6. For example, if the generator protection was to operate within 70μs (corresponding to the time at which a 50% decrease in voltage occurs following a short circuit at F_1), the i^2t threshold would be set to 60A^{2}s. The time to reach this threshold during a higher impedance (1Ω) fault would increase from 2.2ms without the ESS, to 4.5ms when the ESS is operational (a 100% increase in operating time). Furthermore, Table II indicates that operating times for the higher 300A^{2}s trip threshold are increased even further, as the reduced i^2t gradient dominates the change in operating time.

C. Impact of sustained ESS peak current limit on the fault energy output of the generator system

For all fault impedances investigated within section A, the steady state ESS current output reached its limit of 200A. The following case study investigates the impact of applying an ESS peak current limit of 100A – 300A (50% – 150% of the peak generator limit) on the i^2t response of the generator for a fixed fault impedance of 750mΩ. This impedance value is selected as it appears from Fig. 5 that it is the first incremental impedance at which the voltage coupling between the generator system and ESS becomes evident. Fig. 7 illustrates a selection of simulation results that show the i^2t response of the generator system when operating in parallel with the ESS at discrete peak current ratings. These are compared to a baseline trace from when the ESS is disengaged.

Fig. 7 clearly shows that increasing the peak current limit of the ESS relative to that of the generation system serves to reduce the gradient of the generation system i^2t contribution. Moreover, it can be seen that the generator system response is most sensitive to changes in the ESS peak current when this exceed the generation system peak current (i.e. >100%). When the ESS peak current limit is less than that of the generation system (i.e. <100%), the impact on the generation system fault
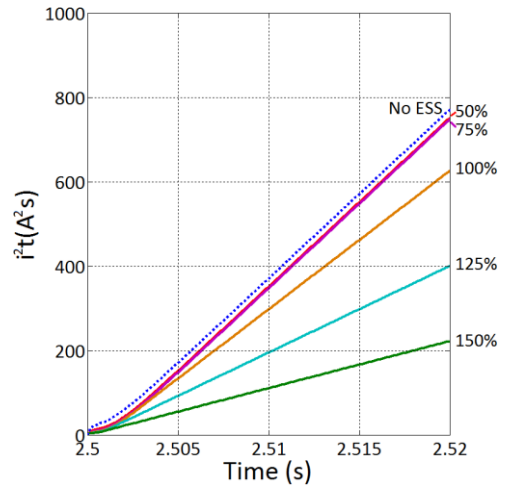
response is more marginal. A reduced discharge of the generator system filter capacitor causes a slight displacement of the generator system output i^2t trace but there is no effect on its steady state output (as indicated by only minor/no changes in the gradient of the corresponding i^2t traces).

Illustrating this further, Table III provides examples of the time-to-threshold that will be expected for the generator system output if particular ESS peak current limits were to be applied. It shows that for both 60A^{2}s and 300A^{2}s threshold levels, there is relatively minimal impact on the generator system current output time-to-threshold for ESS peak current ratings less than the generator system rating. For example, a maximum increase of 0.2ms is observed for the 60A^{2}s threshold whereas an increase of 1.3ms is observed to reach 300A^{2}s. In contrast, notable increases in the time-to-threshold for the generator system are observed when the ESS peak current rating is equal or greater to the generator system. In particular, a threefold increase is noted when the ESS is rated at 150% of the peak current output of the generator system.

D. Impact of ESS bandwidth on the fault energy output of the generator system

The final characteristic considered is the ESS closed-loop bandwidth. Fig. 8 illustrates the fault energy produced by the generation system when the ESS is operating with different closed-loop bandwidths (for a fixed fault impedance of 750mΩ and fixed sustained current output of 200A). The bandwidth of the generation system in this case study is kept constant at 1kHz, whilst the ESS bandwidth is varied logarithmically from 100Hz to 1MHz. A baseline trace where the ESS is inactive is again included for comparison.

Fig. 8 indicates that increasing the bandwidth of the ESS

TABLE II
TIME TO GENERATOR I^{2}T THRESHOLD FOR INCREASING FAULT IMPEDANCE

Fault Impedance at F_1 (mΩ)	Time to 60A^{2}s (no ESS)	Time to 60A^{2}s (with ESS)	Time to 300A^{2}s (no ESS)	Time to 300A^{2}s (with ESS)
1	70μs	70μs	250μs	250μs
100	100μs	150μs	6ms	7ms
500	1.8ms	2.5ms	7.5ms	8.5ms
750	2ms	2.8ms	8ms	10ms
1000	2.2ms	4.5ms	8.2ms	23ms

TABLE III
TIME TO GENERATOR I²T THRESHOLD FOR VARYING ESS PEAK CURRENT
LIMITS AND FIXED FAULT IMPEDANCE (750MΩ)

ESS current limit as a percentage of Gen peak current (%)	Time to 60A²s	Time to 300A²s
No ESS	2ms	8ms
50	2.6ms	8.7ms
75	2.7ms	8.8ms
100	2.8ms	10ms
125	3.4ms	15.2ms
150	5.5ms	27ms

has the effect of introducing an increasing time-delay on the i^2t response of the generator system. For lower ESS bandwidths, corresponding to larger time-constants, the generator system i^2t exhibits a characteristic ripple caused by the discharge of its associated filter capacitor and that of the ESS filter capacitor. As the ESS bandwidth is increased to two orders of magnitude greater than that of the generator system and beyond (i.e. 100-kHz and 1-MHz), the corresponding ripple is smoothed as the ESS time-constant becomes lower than that of the ESS filter capacitor. This eliminates the interaction between both filter capacitors resulting in a smoother discharge of the generator filter capacitor. Accordingly, a maximum shift along the time axis of 900μs is evident at these higher bandwidths in relation to the generator system operating independently.

E. Quantification of network operating and fault conditions under which protection blinding is likely

The effects of the fault impedance and ESS peak current output on the development of the generator system i^2t response can be combined to determine the conditions at which protection blinding becomes evident. Whilst this analysis is system specific, the authors believe the findings are applicable to a wide range of compact DC systems. Fig. 9 depicts a graph of the steady state gradient of the generator system i^2t curve measured when the fault impedance is modified from 1mΩ to 1Ω and the ESS peak current output is adjusted from 50% - 150% of the generator system peak current limit.

Fig. 9 shows that the gradient of the generator output i^2t is consistent for relatively low fault impedances, supporting previous observations. This region of the plot is indicative of the network conditions at which the generator is delivering its peak sustainable fault current. The ESS has thus had little impact on its response compared with the system operating with the ESS disconnected. Alternatively, the region of the surface where the i^2t gradient decreases shows the network conditions where the coupling between the generator system and ESS (through the network voltage) becomes evident, and the response of the generator system to the fault is dampened. Consequently, it is within this region that protection blinding will occur as a result of ESS fault current contribution.

As indicated in [36], the dynamic response of the ESS is dependent on the proportional and integral gain parameters of the voltage control loop for the converter interface. The converter interface will also be limited to how much current it can physically output, according to its rating. A high
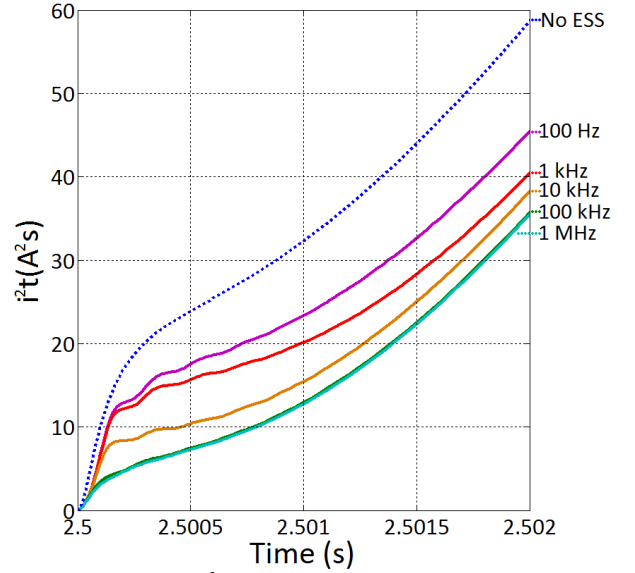

Fig. 8. Generator system i^2t response for varying ESS bandwidth

proportional gain will correspond to a large initial change in the output for a given change in the error, whereas a smaller proportional gain will lead to a less responsive and less sensitive controller. Given that the ESS control system operates directly on the measurement of the network voltage which (during faulted conditions) is analogous to the fault impedance, the ESS current output will likely be driven to its maximum rated limit for a wide range of fault impedances. For increasing levels of fault impedance however, the initial response of the ESS (i.e. the magnitude of current output) will become lower than its rated limit. Therefore, the ESS response will be determined not by the ESS peak current limit but by its controller gain under these faulted conditions. This will have the effect of reducing the gradient of the generator system i^2t to a constant level for a given high impedance fault, independent of the ESS rating. However, this does not affect the impedance at which protection blinding starts to occur as this is still dependent on the peak current limit of the ESS. This can be defined as the critical impedance.

The critical impedance R_c, at which the gradient of the generator system output i^2t will start to decrease (indicating the occurrence of protection blinding) can be estimated as

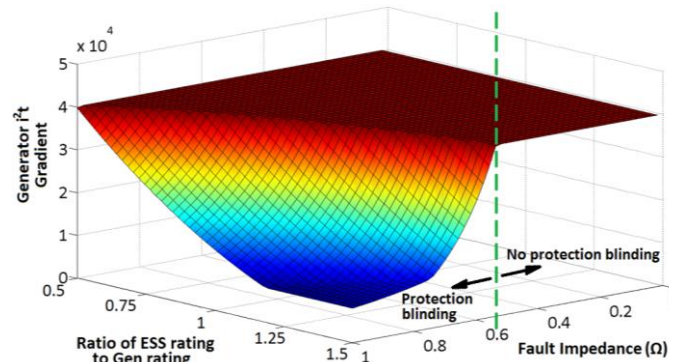$$R_c \approx \frac{v_n}{i_{gen} + i_{ESS}} \tag{1}$$

Fig. 9. Impact of ESS rating and fault impedance on steady state gradient of generator system i^2t response

where v_n is the nominal network voltage, and i_{gen} and i_{ESS} are the maximum sustained currents that the generator system and ESS respectively would supply to a short circuit at their terminals.

The total equivalent impedance R_T of the network during faulted conditions can be estimated as

$$R_T \approx R_e // R_f \tag{2}$$

where R_f is the impedance of the fault itself and R_e is the effective impedance of the network (excluding the fault), and in this case defined as

$$R_e \approx \frac{v_n{}^2}{P_L}. \tag{3}$$

The term P_L is the total load power drawn by the network prior to the fault. If $R_T >> R_c$, the ESS will likely mask the presence of the fault from conventional generator protection devices. Given that R_e (which is determined by the total loading on the network) and R_f are variable, it may be difficult to determine R_T for a suitable range of potential fault conditions. However, it may be possible to determine the minimum possible fault impedance that will cause protection blinding. Under no load conditions, the effective impedance, R_e, will tend to infinity and the total impedance, R_T, will be equivalent to the fault impedance. Therefore, R_c will determine the minimum fault impedance at which protection blinding will occur.

Based on the above approximations, R_c will also provide the conditions for maximum power transfer to a fault. This can be shown by rearranging equation (1) so that

$$\frac{1}{R_c} \approx \frac{i_{gen}}{v_n} + \frac{i_{ESS}}{v_n}. \tag{4}$$

Substituting for the resistance of both sources within (4) gives

$$\frac{1}{R_c} \approx \frac{1}{R_{gen}} + \frac{1}{R_{ESS}}. \tag{5}$$

Within (5) it is apparent that critical resistance, R_c, is the parallel combination of the equivalent internal resistances of the generator system, R_{gen}, and ESS, R_{ESS}, with the internal resistances representing the effects of current control. These are the same conditions for maximum power transfer.

V. DISCUSSION

Altogether, Fig. 5 - 9 and Tables II and III define the degree of protection blinding effects on the primary generation as a result of integrating high bandwidth ESS. It was found that the dominant variable shaping the behavior of the generator system fault response is the ESS peak current rating. A higher ratio between the ESS and generator system ratings will increase the time-to-threshold of conventional protection devices that operate on the i^2t profile of the fault current.

Consequently, if generator protection is set conventionally using only its isolated fault response, it may not be optimized

for all faulted conditions during paralleled operation with the ESS. Depending on the peak current rating of the ESS, the response of the ESS for fault impedances beyond the critical fault impedance (as described by (1)) will temporarily mask the effect of the fault from the generator system. It is under these conditions that the coupling between the sources via the network voltage becomes evident. As a result, overcurrent levels will not be reached as quickly and the speed of the protection system will be reduced. This will expose the wider system to the fault for an extended period and potentially compromise the safety of the power system with increased fire risk at the point of fault. It is plausible that faults of higher impedance, such as arc faults, may induce such behavior. However, the ESS will not influence the dependability and security of the protection system under these conditions.

If instead the i^2t threshold for the generator protection device is set at a lower threshold to reflect the damped response of the generators resulting from ESS operation, coordination issues with downstream protection may occur when the ESS is then disconnected or has a depleted SOC. Under these conditions, the security of the protection system may be reduced.

Thus, it will be difficult to predict how the ESS will respond during network fault conditions, in terms of both the magnitude and duration of fault current contribution, and subsequently how this will impact on the system response as a whole. It is therefore essential to be able to define the acceptable limit of impact (in relative terms) that the ESS will have on the generation system fault response in order to identify where conventional protection approaches are acceptable and where alternative protection approaches are required. The analysis laid out in the previous sections will help to define these limits.

Based on the protection challenges this case study identifies, the following section identifies alternative protection strategies which will help to minimize the impact of energy storage integration on protection system performance.

VI. POTENTIAL PROTECTION SOLUTIONS FOR MORE EFFECTIVE ESS INTEGRATION

Two main solution types are considered. First, the section will consider how a network could make use of adaptive settings to improve an overcurrent scheme's response. The subsequent section then discusses how communication based protection methods could provide a means of safely integrating ESS onto a compact power system.

A. Adaptive Protection for the Generator Protection Devices

Adaptive protection is a well-established method that can enable the effective protection of power systems that are reconfigurable or change operating state. Adaptive protection operates on the principle of utilizing distinct or variable protection relay settings that can be selected depending on predefined network states [39]. As such, this approach may be suitable for the protection of the generator system operating in parallel with an ESS.

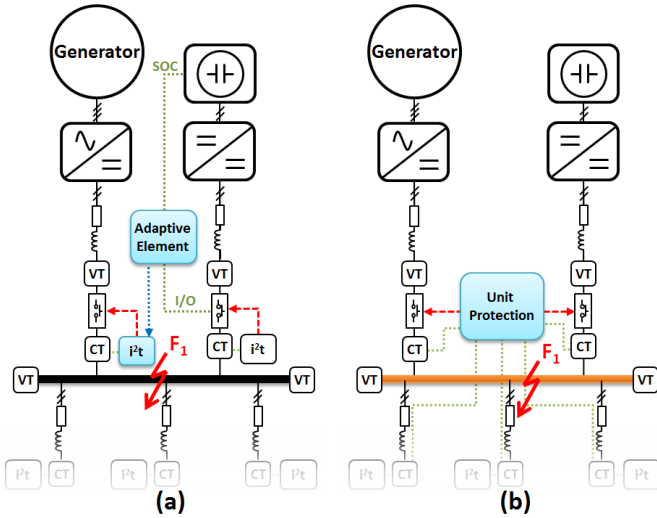Given the distinctive response of the primary source of

Fig. 10. (a) Adaptive protection and (b) bus-bar unit protection configuration

TABLE IV
TIME TO GENERATOR I^2T THRESHOLD FOR ADAPTED SETTINGS

R_f at F_1 (mΩ)	Time to threshold					
	$60A^2s$ (no ESS)	$60A^2s$ (with ESS)	$40A^2s$ (with ESS)	$300A^2s$ (no ESS)	$300A^2s$ (with ESS)	$250A^2s$ (with ESS)
1	70µs	70µs	60µs	250µs	250µs	200µs
100	100µs	150µs	100µs	6ms	7ms	5.8ms
500	1.8ms	2.5ms	1.9ms	7.8ms	8.5ms	7.5ms
750	2ms	2.8ms	2.1ms	8ms	10ms	8.5ms
1000	2.2ms	4.5ms	3.1ms	8.2ms	23ms	18ms

generation to a fault at F_1 when the ESS is operational and when it is disconnected, one option would be to select two distinct settings for the primary generator protection. When the ESS is disengaged from the network or the ESS SOC is depleted to a level that will render it incapable of impacting the generator performance, the generator overcurrent relay may be set using the conventional isolated fault response. This would then be adjusted to a predetermined lower setting when the ESS is activated and is operating normally. These overcurrent protection settings can be updated using an adaptive element as Figure 10(a) illustrates.

To demonstrate the impact this approach can have on protection operating time, Table IV presents a selection of simulation results that show the time-to-threshold performance of the generator overcurrent protection device when reduced threshold settings are selected for when the ESS is connected. The results in Table IV show that for an i^2t threshold of $40A^2s$ in place of $60A^2s$ for when the ESS is operational, the time-to-threshold for the majority of selected fault impedances are within 1ms of the desired operating times. However, it is difficult to exactly match the response times for both network states and all potential fault impedances. This is accentuated at higher trip thresholds, where a 10ms difference is observed for a 1Ω fault when the threshold is adapted from $300A^2s$ to $250A^2s$ when the ESS is engaged.

The performance of the adaptive scheme may be improved through the use of a wider range of discrete settings. However note that further reduction in thresholds for when the ESS is operational may result in reduced coordination with downstream devices.

Similar adjustments to protection settings may be made depending on the operational state of bus ties and other configurable sections if the protection system is employed in a more complex network topology. However, any such scheme would also require the use of a larger communications network between the ESS, configuration contactors, generator systems and their corresponding protective devices and would therefore be more complex and costly.

B. Bus-Bar Unit Protection

A unit protection system [15,16,37] may accommodate ESS behavior and address some of the integration challenges associated with such sources. This type of protection system can be implemented on a network by summing measurements of current from all sources and loads connected to the common bus bar, as illustrated in Figure 10(b). By being largely insensitive to fault current magnitude, a unit protection scheme would also be insensitive to ESS connection status. Additionally, the highly selective principle of unit protection will enable the optimal response of the ESS for close up faults. This would prevent the ESS from unnecessarily adding to the energy delivered at the point of fault, thus preventing the dissipation of additional energy stored within the ESS, and increasing the ability of this system to support the post-fault recovery of the network and its loads.

The key drawback of such methods however is the lack of provision of backup protection functionality. This would have to be provided through convention overcurrent approaches (which may be enhanced by the adaptive protection philosophy described previously). Additionally, as with the adaptive protection, this solution would also be heavily reliant on communications with similarly associated drawbacks.

VII. CONCLUSIONS

While high bandwidth ESS can increase the operational capability and overall flexibility of a power system, understanding its impact on the existing network protection systems is essential to ensure its safe integration. This paper has identified that the peak current rating of the ESS is a key characteristic that will determine the extent of the protection blinding effects. For fault impedances beyond that of the identified critical value, the ESS has been shown to dampen the fault response of slower acting generator systems. It is speculated that key behavioral trends may be applicable to wider applications containing multiple generators and/or ESSs. The paper has also demonstrated the limitations of existing protection solutions through modeling and simulation and identified more suitable protection approaches to remove/minimize the effects of protection blinding. Beyond this, the authors plan to further explore and evaluate existing and novel network-wide protection methods in order to establish a framework that provides the criteria for effectively achieving fast and discriminatory protection for the primary generation when operating in parallel with an ESS.

REFERENCES

[1] D. Rastler, "Electricity Energy Storage Technology Options: A White Paper on Applications, Costs, and Benefits", *EPRI*, December 2010

[2] F. A. Inthamoussou, J. Pegueroles-Queralt, and F. D. Bianchi, "Control of a Supercapacitor Energy Storage System for Microgrid Applications," *IEEE Trans. Energy Convers.*, vol. 28, 2013.

[3] L. Xu and D. Chen, "Control and Operation of a DC Microgrid With Variable Generation and Energy Storage," *IEEE Trans. Power Del., vol.26, no.4, pp.2513-2522, Oct.* 2011.

[4] S. Vazquez, S. M. Lukic, E. Galvan, L. G. Franquelo, and J. M. Carrasco, "Energy Storage Systems for Transport and Grid Applications," *IEEE Trans. Ind. Electron.*, vol. 57, pp. 3881-3895, 2010.

[5] S. Samineni, B. K. Johnson, H. L. Hess, and J. D. Law, "Modeling and analysis of a flywheel energy storage system for Voltage sag correction," *IEEE Trans. Industry App.*, vol. 42, pp. 42-52, 2006.

[6] I. M. Elders, J. D. Schuddebeurs, C. D. Booth, G. M. Burt, and J. . McDonald, "Energy Storage Systems as a Mechanism for Improving Power Quality in an IFEP System," presented at the 9th Intl Naval Engineering Conference, April 2008.

[7] B. Zahedi and L. E. Norum, "Modeling and Simulation of All-Electric Ships With Low-Voltage DC Hybrid Power Systems," *IEEE Trans. Power Electron.*, vol. 28, pp. 4525-4537, 2013.

[8] H. Zhang, F. Mollet, C. Saudemont, and B. Robyns, "Experimental Validation of Energy Storage System Management Strategies for a Local DC Distribution System of More Electric Aircraft," *IEEE Trans. Ind. Electron.*, vol. 57, pp. 3905-3916, 2010.

[9] A. Jaafar, C. R. Akli, B. Sareni, X. Roboam, and A. Jeunesse, "Sizing and Energy Management of a Hybrid Locomotive Based on Flywheel and Accumulators," *IEEE Trans. Veh. Technol.*, vol. 58, pp. 3947-3958, 2009.

[10] P. Rakhra, P. J. Norman, S. D. A. Fletcher, S. J. Galloway, and G. M. Burt, "A Holistic Approach Towards Optimizing Energy Storage Response during Network Faulted Conditions within an Aircraft Electrical Power System," *SAE Int. J. Aerosp. 5(2):548-556, 2012.*

[11] P. Rakhra, P. J. Norman, S. D. A. Fletcher, S. J. Galloway, and G. M. Burt, "Toward optimising energy storage response during network faulted conditions within an aircraft electrical power system," in *Electrical Systems for Aircraft, Railway and Ship Propulsion (ESARS), 2012*, .

[12] F. Coffele, C. Booth, A. Dysko, and G. Burt, "Quantitative analysis of network protection blinding for systems incorporating distributed generation," *IET Generation, Transmission & Distribution*, vol. 6, pp. 1218-1224, 2012.

[13] D. Salomonsson, L. Soder, and A. Sannino, "Protection of Low-Voltage DC Microgrids," *IEEE Trans. Power Del.*, vol.24, no.3, pp.1045-1053, July 2009.

[14] S. D. A. Fletcher, P. J. Norman, S. J. Galloway, and G. M. Burt, "Determination of protection system requirements for dc unmanned aerial vehicle electrical power networks for enhanced capability and survivability," *IET Electrical Systems in Transportation*, vol. 1, pp. 137-147, 2011.

[15] Fletcher, S.D.A.; Norman, P.J.; Galloway, S.J.; Crolla, P.; Burt, G.M., "Optimizing the Roles of Unit and Non-unit Protection Methods Within DC Microgrids," *IEEE Trans. Smart Grid*, vol.3, no.4, pp.2079-2087, Dec. 2012

[16] Fletcher, S.D.A.; Norman, P.J.; Fong, K.; Galloway, S.J.; Burt, G.M., "High-Speed Differential Protection for Smart DC Distribution Systems," *IEEE Trans. Smart Grid*, vol.5, no.5, pp.2610.-2617, Sept. 2014

[17] Elserougi, A.A.; Abdel-Khalik, A.S.; Massoud, A.M.; Ahmed, S., "A New Protection Scheme for HVDC Converters Against DC-Side Faults With Current Suppression Capability," *IEEE Trans. Power Del.*, vol.29, no.4, pp.1569-1577, Aug. 2014

[18] Xiaoqian Li; Qiang Song; Wenhua Liu; Hong Rao; Shukai Xu; Licheng Li, "Protection of Nonpermanent Faults on DC Overhead Lines in MMC-Based HVDC Systems," *IEEE Trans. Power Del.*, vol.28, no.1, pp.483-490, Jan. 2013

[19] Jin Yang; Fletcher, J.E.; O'Reilly, J., "Multiterminal DC Wind Farm Collection Grid Internal Fault Analysis and Protection Design," *IEEE Trans. Power Del.*, vol.25, no.4, pp.2308-2318, Oct. 2010

[20] Jae-Do Park; Candelaria, J.; Liuyan Ma; Dunn, K., "DC Ring-Bus Microgrid Fault Protection and Identification of Fault Location," *IEEE Trans. Power Del.*, vol.28, no.4, pp.2574-2584, Oct. 2013

[21] Baran, M.E.; Mahajan, N.R., "Overcurrent Protection on Voltage-Source-Converter-Based Multiterminal DC Distribution Systems," *IEEE Trans. Power Del.*, vol.22, no.1, pp.406-412 Jan. 2007

[22] Ke Jia; Christopher, E.; Thomas, D.; Sumner, M.; Tianshu Bi, "Advanced DC zonal marine power system protection," *IET Generation, Transmission & Distribution*, vol.8, no.2, pp.301-309, February 2014

[23] Jovcic, D.; Taherbaneh, M.; Taisne, J.-P.; Nguefeu, S., "Offshore DC Grids as an Interconnection of Radial Systems: Protection and Control Aspects," *IEEE Trans. Smart Grid*, vol.6, no.2, pp.903-910, March 2015

[24] Uriarte, F.M.; Gattozzi, A.L.; Herbst, J.D.; Estes, H.B.; Hotz, T.J.; Kwasinski, A.; Hebner, R.E., "A DC Arc Model for Series Faults in Low Voltage Microgrids," *IEEE Trans. Smart Grid*, vol.3, no.4, pp.2063-2070, Dec. 2012

[25] D. R. Doan, "Arc Flash Calculations for Exposures to DC Systems," *IEEE Trans Ind App, ,* vol. 46, pp. 2299-2302, 2010.

[26] Cairoli, P.; Dougal, R.A., "New Horizons in DC Shipboard Power Systems: New fault protection strategies are essential to the adoption of dc power systems..," *Electrification Magazine, IEEE* , vol.1, no.2, pp.38-45, Dec. 2013

[27] Schmerda, R.; Cuzner, R.; Clark, R.; Nowak, D.; Bunzel, S., "Shipboard Solid-State Protection: Overview and Applications," *Electrification Magazine, IEEE* , vol.1, no.1, pp.32-39, Sept. 2013

[28] Izquierdo, D.; Barrado, A.; Fernández, C.; Sanz, M.; Zumel, P., "Behavioral model for solid-state power controller," IEEE Aerosp. Electron. Syst. Mag. , vol.28, no.12, pp.4-11, Dec. 2013

[29] A. Khaligh and L. Zhihao, "Battery, Ultracapacitor, Fuel Cell, and Hybrid Energy Storage Systems for Electric, Hybrid Electric, Fuel Cell, and Plug-In Hybrid Electric Vehicles: State of the Art," *IEEE Trans. Veh. Technol.*, vol. 59, pp. 2806-2814, 2010.

[30] Ivanovic, Z.R.; Adžić, E.M.; Vekić, M.S.; Grabić, S.U.; Čelanović, N.L.; Katić, V.A.,., "HIL Evaluation of Power Flow Control Strategies for Energy Storage Connected to Smart Grid Under Unbalanced Conditions," *IEEE Trans. Power Electron.*, vol. 27, pp. 4699-4710, 2012.

[31] L. Corradini, P. Mattavelli, E. Tedeschi, and D. Trevisan, "High-Bandwidth Multisampled Digitally Controlled DC-DC Converters Using Ripple Compensation," *IEEE Trans. Ind. Electron.*, vol. 55, pp. 1501-1508, 2008.

[32] L. Ruqi, T. O'Brien, J. Lee, and J. Beecroft, "A unified small signal analysis of DC-DC converters with Average Current Mode Control," in *IEEE Energy Conversion Congress and Exposition*, pp. 647-654, 2009.

[33] B. J. Arnet and L. P. Haines, "High power DC-to-DC converter for supercapacitors," in *Electric Machines and Drives Conference,. IEEE International*, pp. 985-990, 2001.

[34] R. Todd and A. J. Forsyth, "DC-bus power quality for UAV systems during generator fault conditions," in *Power Electronics, Machines and Drives, 5th IET International Conference on*, 2010,.

[35] M. Won-Sik, W. Jong-Nam, H. Jae-Sun, and K. Jae-Chul, "A Study on the Application of a Superconducting Fault Current Limiter for Energy Storage Protection in a Power Distribution System," *IEEE Trans. Appl. Supercond.*, vol. 23, no. 3, article no. 5603404, 2013.

[36] X. Guoyi, X. Lie, D. J. Morrow, and C. Dong, "Coordinated DC Voltage Control of Wind Turbine With Embedded ESS" *IEEE Trans. Energy Convers.*, vol. 27, pp. 1036-1045, 2012.

[37] *Network Protection and Automation Guide*: Alstom Grid, 2011.

[38] (2010). *MATLAB & SIMULINK: version (R2010a. ed.)*.

[39] G. D. Rockefeller, C. L. Wagner, J. R. Linders, K. L. Hicks, and D. T. Rizy, "Adaptive transmission relaying concepts for improved performance," *IEEE Trans. Power Del.*, vol. 3, pp. 1446-1458, 1988.

[40] Haj-ahmed, M.; Illindala, M., "Investigation of Protection Schemes for Flexible Distribution of Energy and Storage Resources in an Industrial Microgrid," *IEEE Trans. Ind. Appl.*, online access, October 2014

[41]   G.E. Alexander, J.G. Andrichak, S.D. Rowe, "Evaluating Line Relaying Schemes in Terms of Speed, Security and Dependability," *GE Power Management,* 1998

Puran Rakhra received his MEng degree in electrical and mechanical engineering from the University of Strathclyde, Glasgow, U.K in 2010. He is currently pursuing his Ph.D. in electrical engineering from the University of Strathclyde. His research interests include aerospace electrical power systems, power system protection and energy storage integration.

Patrick Norman is a lecturer within the Institute for Energy and Environment at the University of Strathclyde. He received his BEng (Hons) degree in electrical and mechanical engineering and Ph.D. in electrical engineering from the University of Strathclyde. His research interests lie in the modelling and simulation, design, control, protection of aircraft secondary power offtake and distribution systems, microgrid and shipboard power systems.

Steven Fletcher (M'13) received his BEng degree in electrical and electronic engineering from the University of Strathclyde, Glasgow, U.K in 2007 and his Ph.D. degree from University of Strathclyde in 2013, following research into dc network protection. He is currently a research associate within the Institute for Energy and Environment at Strathclyde. His research interests include the design, modelling and protection of microgrid, marine and aerospace power systems.

Stuart Galloway received his Bachelors degree in Mathematical Sciences form the University of Paisley in 1992. He obtained his M.Sc. degree in Non-linear Modelling (1993) and Ph.D. in Numerical Analysis (1998) from the University of Edinburgh, UK. Since 1998 he has been researching optimisation problems in power systems, electricity markets and novel architectures relating to aero and marine electrical systems. He is currently a Reader in the Institute for Energy and Environment at the University of Strathclyde.

Graeme M. Burt (M'95) received the B.Eng. degree in electrical and electronic engineering from the University of Strathclyde, Glasgow, UK, in 1988, and the Ph.D. degree from the University of Strathclyde in 1992, following research into fault diagnostic techniques for power networks. He is currently a Director of the Institute for Energy and Environment at the University of Strathclyde, where he also directs the University Technology Centre in Electrical Power Systems sponsored by Rolls-Royce. He is a professor of electrical power engineering, and has research interests in the areas of: integration of distributed generation; power system modelling, real-time simulation, protection and control; microgrids and more-electric systems.